Proceedings of 15th International Marine Design Conference (IMDC-2024)
June 2-6, 2024
Amsterdam, the Netherlands

Integration of the Power Corridor Concept in the Early-Phase Design of Electric Naval Ships using Mathematical Design Models

Giorgio Trincas[1], Luca Braidotti[1,*] Andrea Vicenzutti[1], Andrea Alessia Tavagnutti[1], Chathan M. Cooke[2], Julie Chalfant[2], Vittorio Bucci[1], Chryssostomos Chryssostomidis[2] and Giorgio Sulligoi[1]

ABSTRACT

The aim of this paper is to illustrate the process of identifying the 'best compromise' solution for an all-electric destroyer at the concept design level. The design strategy reflects a paradigm shift from a sequential approach towards a holistic multicriterial approach. The destroyer is required for an extensive range and endurance, fully operable in rough sea states. A mathematical design model (MDM) that includes a set of metamodels, is implemented to evaluate the overall performance of feasible, then non-dominated designs. The power corridor concept is integrated into the MDM to optimize the location and functionality of the individual units of the power train. The fuzzy sets theory is used for normalizing and weighing incommensurable properties of candidate designs, so resolving many of the ill-defined requirements and criteria. The final result of this study is a top-level specification for the destroyer with enhanced performance and reduced power demand.

KEY WORDS

Concept ship design; destroyer; all-electric ship; power corridor; fuzzy-sets

NOMENCLATURE

Symbols

A_X	area of maximum section area
B_{MAX}	beam, maximum
B_{WL}	beam at design draft
BM	transverse metacentric radius
BM_L	longitudinal metacentric radius
C_B	block coefficient at design draft
C_{BD}	block coefficient at ship deck
$C_{GM/B}$	stability coefficient
C_{WP}	waterline area coefficient
C_P	longitudinal prismatic coefficient
C_{VP}	vertical prismatic coefficient
C_{WP}	waterline area coefficient
C_X	wind resistance coefficient
D_P	propeller diameter
D_{tac}	tactical diameter

Acronyms

AAC	annual average cost
AC	alternating current
AS	attribute space
DC	direct current
$DESMAD$	destroyer multiattribute design
DOE	design of experiments
$DTMB$	David Taylor Model Basin
DWT	deadweight
DS	design space
$HVAC$	heating, ventilation, air conditioning
IMO	International Maritime Organization
$ITTC$	International Towing Tank Conference
LSW	lightship weight
$MADM$	multiattribute decision-making
$MCDM$	multicriterial decision-making

[1] Department of Engineering and Architecture, University of Trieste, Italy
[2] Massachusetts Institute of Technology, 77 Massachusetts Ave, Cambridge, MA 02139, USA
* Corresponding Author: lbraidotti@units.it

Submitted: 23 February 2024, Revised: 30 April 2024, Accepted: 1 May 2024, Published: 6 May 2024

Conference paper, DOI: https://doi.org/10.59490/imdc.2024.753 e-ISSN: 3050-4864

GM	metacentric height
$H_{1/3}$	significant wave height
i_E	entrance half-angle
KB	vertical center of buoyancy
KG	vertical center of mass
KM	metacentric height from baseline
KQ	propeller torque coefficient
KT	propeller thrust coefficient
LCB	longitudinal center of buoyancy
L_{PC}	length for future power corridor
T_ϕ	natural roll period
V_{MAX}	maximum ship speed
S_ζ	spectral value of the sea
W_{FL}	full load weight
W_{HS}	hull steel weight
W_{PL}	payload weight
α_{cut}	threshold for fuzzy attributes
μ	membership grade function
ρ_a	air density
ζ_a	wave amplitude
ω_e	encounter frequency
Δ	full load displacement
∇	volume of displacement
MCR	maximum continuous rating
MDM	mathematical design model
MDO	marine diesel oil
MIT	Massachusetts Institute of Technology
$MODM$	mathematical design model
MOP	measure of seakeeping performance
MSI	motion sickness incidence
MVZ	main vertical zones
NA	number of attributes
ND	number of non-dominated designs
$NORDFORSK$	Nordic Co-operative Organization for Applied Research
NV	number of variables
$PEBB$	power electronics building blocks
RMS	root-mean-square
RSM	response surface methodology
$STANAG$	standardization agreement
$SWBS$	ship work breakdown system
$UNITS$	University of Trieste
VLS	vertical launch system
$ZEDS$	zonal electric power distribution system

INTRODUCTION

The modern destroyer, born in response to the threat posed by torpedo boats to larger fleet vessels at the end of the 19th century, has evolved into a highly versatile and heavily armed surface unit. It is capable of escorting naval groups and merchant convoys, conducting anti-submarine operations, and engaging in air and surface combat with missiles, electronic warfare, and counter missions. Despite the vague classification between frigates and cruisers, destroyers often represent the most dominant surface units in the fleets of major navies.

In recent decades, there has been a steady increase in the size of naval vessels, and destroyers are no exception. Displacement and length have surpassed 10,000 tons and 160 meters, respectively, with vessels like the Zumwalt of the US Navy reaching 14,564 tons and 182.8 meters. This growth is driven by the escalating power demands of new sensors and onboard systems, as well as by the anticipated introduction of disruptive technologies such as direct energy weapons and railguns, currently under development or testing by several navies. These advancements underscore the heightened focus on the onboard electric power system, its architecture, and its arrangement. Specifically, there are increased requirements for safety, redundancy, and modularity to enhance ship survivability and facilitate retrofits and upgrades throughout the ship's operational lifespan, especially on full-electric ships.

To face these challenges, the main scope of this paper is to develop an innovative design approach for an all-electric destroyer where the integration of a power corridor plays a fundamental role in concept design and decision-making processes. This poses increasing challenges to naval ship design, which has to find new solutions and arrangements to cope with the increasing space and power demand (and thus, installed power, amount of fuel, etc.).

Destroyers are fast warships intended to escort larger vessels and equipped for antisubmarine warfare, with missiles for surface and air combat, as well as for electronic warfare. The new destroyer will have to guarantee high-level operability from the conceptual design phase, taking into account the following basic factors:

- the hydrodynamic quality of the ship hull, and the interaction of equipment, subsystems, and military installations between them and the ship body;
- the hull-environment interaction in rough sea states
- a set of crisp and soft criteria to be satisfied which respect all requirements of physical and normative nature.

To include simultaneously all these factors, it is necessary to change the paradigm in the ship design process. A multicriterial approach in ship design is the best answer for overcoming heuristic approaches such as the classic design spiral. In particular, more than the multiobjective design method, the multiattribute decision-making approach was found to be the most suitable for the concept design (Triantaphyllou, 2000; Trincas, 2001; Trincas et al., 2018). The theory of fuzzy sets was incorporated into the decision-making procedure to provide a simple mathematical tool to handle uncertainty and imprecision in the concept design phase.

Decades of experience on naval ships have shown that the order of importance to attach to the various hydrodynamic disciplines is seakeeping first, then stability and control both in the vertical plane and in maneuvering, then propulsion, and finally resistance. To respond to this scale of priorities right from the concept design, it is necessary to develop seakeeping metamodels to rapidly evaluate responses in a seaway while ensuring ship safety.
To define the new compartmental configuration with a deck dedicated to the power corridor with systems and equipment it contains, reference is made to the seminal papers of Nehrling (1985) and Cort & Williams (1987).
The paper has seven main sections. Section 2 illustrates the concept design strategy based on the principles of the multiattribute decision-making process. Section 3 describes the main feature of the power corridor designed to satisfy the destroyer's overall energy requirement. Section 4 describes the main modules that make up the mathematical design model. Section 5 deals with the decision support system where the attributes' outcomes are fuzzified. Section 6 develops the design of the baseline destroyer as an anchor point for competing designs. Section 7 contains the two phases of the multiattribute decision making process: generations of feasible designs and selection of the preferred design. Finally, section 8 draws some conclusions.

METHODOLOGY

Ship Design Methods

Successful engineering design, including ship design, is mainly a matter of fast and efficient decision-making in a conflicting environment. This is especially worthwhile for concept design, which is the most important phase of the global design process since it gives the highest opportunity to influence the overall efficiency and effectiveness of the ship a long way ahead. Even though evaluation of design alternatives requires rational decision-making, so far the usual way is still to reduce target complexity by using a heuristic approach in order to arrive at final technical decisions. Major weak points and ineffectiveness of still popular design methods mainly relate to the poor integration of different subsystems and the lack of mutual influence of design responses to different requirements.
Design theory has evolved to evaluate design alternatives in an integrated shell rationally, where multiple conflicting requirements, external environments, and mandatory rules are to be tackled simultaneously. This limit was overcome by the development of the multiple criteria decision-making (MCDM), which was also the name of the first conference on the subject held at the University of South Carolina in 1972. The basic concepts (optimization, satisficing solution, compromising set, ideal solution) of the MCDM can be found in the fundamental work of Zeleny (1982).
A profound debate conducted in the 1990s between naval experts and researchers, especially during IMDC and PRADS conferences, led to the distinction between multiple attribute decision-making (MADM) and multiple objective decision-making (MODM), different in application scope and underlying mathematical approach. The generally accepted conclusions were that the MADM approach is more suitable for the concept design phase (where analytical mathematics is generally used), while the MODM approach is recommended in the preliminary/contractual design phase when it comes to optimizing ship systems and subsystems. Trincas et al. (2018) summarized the impossibility of applying MODM methodologies in the concept design stage, also supported by the conclusions of recognized naval field MODM experts: Campana et al. (2007) among others. Therefore, the aim of this work is not to confirm the validity of the MADM methodology in developing a concept ship design, but to use it to propose a feasible project of an innovative all-electric naval vessel based on the power corridor concept.

Concept Design Modeling

Many design teams forego a concept design altogether and proceed directly to the preliminary design phase. They usually follow the iterative design spiral procedure although mostly not in a formal way. Firstly, main dimensions are determined on a statistical basis; then a lines plan is developed and the general arrangement plan is fitted in. Hydrostatics and stability assessment, overall power estimate, engine selection, strength evaluation, seakeeping and manoeuvring qualities then follow from the analytical/numerical procedures applied to the single lines plan. A tedious trial and error process brings the relevant features of the design in balance. Such a design process is time-consuming, as no complete definition of the ship exists before a balance is reached at each turn of the design spiral.
The concept design is not a substitute for the traditional preliminary design; rather, it should precede it, yielding a top-level specification based on the primary characteristics and performance requirements of the preferred design. This early design stage has the aim of avoiding a redesign in a later stage, as often is necessary with descriptive methods (Trincas et al., 1994; Hubka and Eder, 1996) in ship design. The concept design is conceived as a new paradigm where the key words are selection, concurrency and multidimensional design space. The early phase of the ship design process requires reliable and fast time decisions, allowing the design team to explore a wide range of feasible solutions and offering increased assurance for benefits throughout the ship's lifetime. Such a demand requires that several fundamental features, normally associated with later phases of the design process, should be anticipated at the level of concept design. In the present study, one of these features is the

integration of the power corridor into the general arrangement plan and evaluation of its effect on the optimal choice of the main characteristics of the destroyer (ship dimensions, general plans, hydrodynamic properties).
The concept design process follows a prescriptive model (Andreasen, 1992) that is broken down into three basic interrelated activities:

- *design analysis*: random generation and performance assessment of a large number of design alternatives that have to meet the required targets subject to crisp and soft constraints; this activity is performed by executing the mathematical design model so many times as to fill the design space enough;
- *design synthesis*: filtering the feasible designs (i.e., designs not eliminated automatically by crisp constraints); creating the set of non-dominated designs that constitute the Pareto frontier;
- *design selection*: based on different metrics and multiple attribute decision-making techniques, aimed at selecting the preferred design from the ones in the Pareto frontier.

The quality and accuracy of the *design analysis* is crucial, since it dramatically affects the target of obtaining a successful ship. Unfortunately, at concept design stage the design team is often faced with imprecise information on the functional requirements and uncertainties in the ship performance, as well as with the significant interaction and interconnectivity of the main ship design disciplines. All these aspects make ships complex systems that requires highly evolved decision tools to handle this high degree of complexity. Since it becomes impractical to rely on simulation and numerical codes for the purpose of concept design, a preferable strategy is to use approximation models, which are referred as metamodels as they provide a 'model of the model' (Kleijen, 1987), to replace the expensive detailed simulation models. A metamodel-based approach (i.e., artificial intelligence applied to ship design) is the solution also to limit uncertainties across the predicted performance, functional requirements, building costs, and so forth (Derelöv, 2009), while reducing the computational expense and the design cycle time, and providing quick tradeoff for evaluation. Evaluation (*design synthesis*) and decision making (*design selection*) are key parts of the design process. In conventional ship design they are generally poorly structured and depend significantly on designers' own perceptions, which often imply a subjective (and thus suboptimal) assessment as a result. To improve on the latter, the Authors propose an evaluation strategy that combines a MADM approach (Trincas et al., 1994; Pahl et al., 1996) with different techniques (feasibility judgement, ELECTRE method and Pareto frontier), to reduce the number of candidate solutions (Ulrich and Eppinger, 2007).

POWER CORRIDOR

Cooke et al. (2017) introduced the concept of Power Corridor: a single entity incorporating distribution, conversion, isolation and storage of main bus power throughout the ship. The aim was to introduce significant advantages in terms of higher level of survivability, a simplified general arrangement plan of the ship as well as reduction of building and life-cycle costs.
Thanks to the on-land construction of the power corridor modules, and the subsequent easy onboard assembly, the cost of initial construction and repair (and future modernization) of the power corridor will be reduced compared to standard onboard power plants. Advantages in terms of standardization in modules' production (e.g., power electronics converters based on the Power Electronics Building Blocks – PEBB – concept) and the possibility to de-risk new modules in the factory are also present. Thus, a reduction in production, installation, supply chain, and training costs is expected. The use of identical pieces of hardware and control interfaces rather than many bespoke units also provides improved maintainability.
The installation of two redundant power corridors, installed onboard in separated locations, together with the centralization of the distribution, isolation, and energy storage functions, provides improved survivability. The interchangeability of the power corridor modules enables fast and easy replacement of faulted elements during service (without requiring ship docking).
The definition of a single entity dedicated to most of the functions related to electric power generation, distribution, and utilization, provides advantages in terms of quality of the ship design. In fact, the onboard arrangement can benefit from the Reserved Space approach, where the length and volume dedicated to the power corridor can be defined in the early phases of the ship design (Chalfant, 2015). This simplifies the process of allocating onboard the power system components, leading to the possibility of considering the power system design of an all-electric ship much earlier in the ship design process, enhancing the design results. This is because it encourages the ship's design team to consider the power system as an integral part of the ship design, optimizing it dually in relation to the overall ship. The use of uniform modules also aids in this regard.
A representation of the Power Corridor is depicted in Figure 1. It is composed of the following main components:

- bus cable and conduit (magenta)
- power converter stack (dark blue and brown)
- interface junction box (orange)
- energy storage (salmon)
- circuit breaker or disconnect (teal)
- bulkhead penetration (gray)

The details about the Power Corridor concept can be found in Cooke et al. (2017).

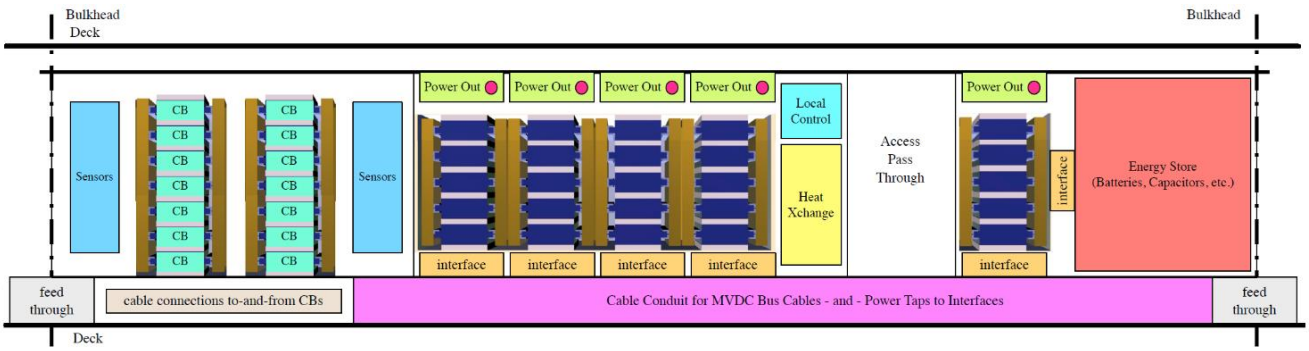

Figure 1: Modular integrated power corridor (Cooke et al., 2017)

The Power Corridor concept briefly presented above is here used as a key point in the design process. Thanks to its modular nature, it enables the integration of critical components of the power system directly into the concept mathematical design model, thus expanding its capabilities. The expected result is the definition of a set of feasible ship designs, evaluated considering not only the usual ship design parameters and constraints, but also the electrical related ones (power, space, weight, cooling, etc.).

MATHEMATICAL DESIGN MODEL

Ship properties that are likely to influence the identification of viable alternatives and their selection must be determined and analyzed as early as possible, that is, at the concept design phase. In fact, the success of the decision-making process in the concept design depends on how effectively the mathematical design model (MDM) simulates the real performance of the ship taking into account a sufficient number of primary properties (attributes). The MDM yields a large set of alternative solutions that have to be feasible in terms of the selected attributes. The candidate designs are randomly generated employing an adaptive Monte Carlo method. The structure of MDM is modular to allow the design team to vary or include different sets of analytical formulations and data to model the problem at hand with the greatest possible accuracy. It contains various design relationships for calculating areas, volumes, sizes, weights, electric power, stability, and so forth.
The MDM employs relationships based on practical design skills, scientific-based methods and metamodels based on statistical analysis of databases of similar ships, e.g. destroyers. It is written in Fortran 90 language.

Structure of the Model

The general structure of the MDM for destroyers, denoted as DESMAD and described in Figure 2, evaluates the attributes by a number of analytical modules, some of which consist of metamodels.
Unlike other mathematical models developed by various naval design centres, DESMAD does not include any iterative process except in the hull steel weight module. The approach adopted is non-compensatory: if a candidate design does not overcome any crisp constraint of geometric, physical and/or regulatory nature, it is immediately discarded. Only the designs in which both primary and secondary attributes overcome the constraints are feasible and are stored in the decision matrix.

Hullform Definition

This module selects the hull dimensions and relationships, which determine the technical requirements and capabilities of the candidate designs. The choice of appropriate form parameters has to comply with many constraints, mainly related to main dimensions and longitudinal prismatic coefficient. One crisp constraint is to have a natural roll period higher than 10 seconds to avoid the installation of large anti-rolling devices. As capability to sustain medium-high speed in rough weather and good ride quality are desired targets, a slender hullform is mandatory. The design waterline must have an entrance half-angle below 10 degrees. V-shaped sections are recommended even if at the expense of a slight extra building cost. In order to reach high efficiency at high speeds with minimum pressure pulses against the hull from the propellers, a hull/tip clearance not lower than 25 percent of the propeller diameter is imposed.
In each generation, some geometrical characteristics, such as C_B and $C_{WP} = C_B/C_{VP}$ are immediately derivable from the independent variables. For this purpose, starting from four basic hulls and using the Box-Behnken four-level design DoE technique (Myers et al., 2016) a database of one hundred hulls was constructed whose geometric characteristics of interest (BM, BML, KB, WS, LCB, LCF) were determined by statistical analysis with the Response Surface Methodology (RSM).

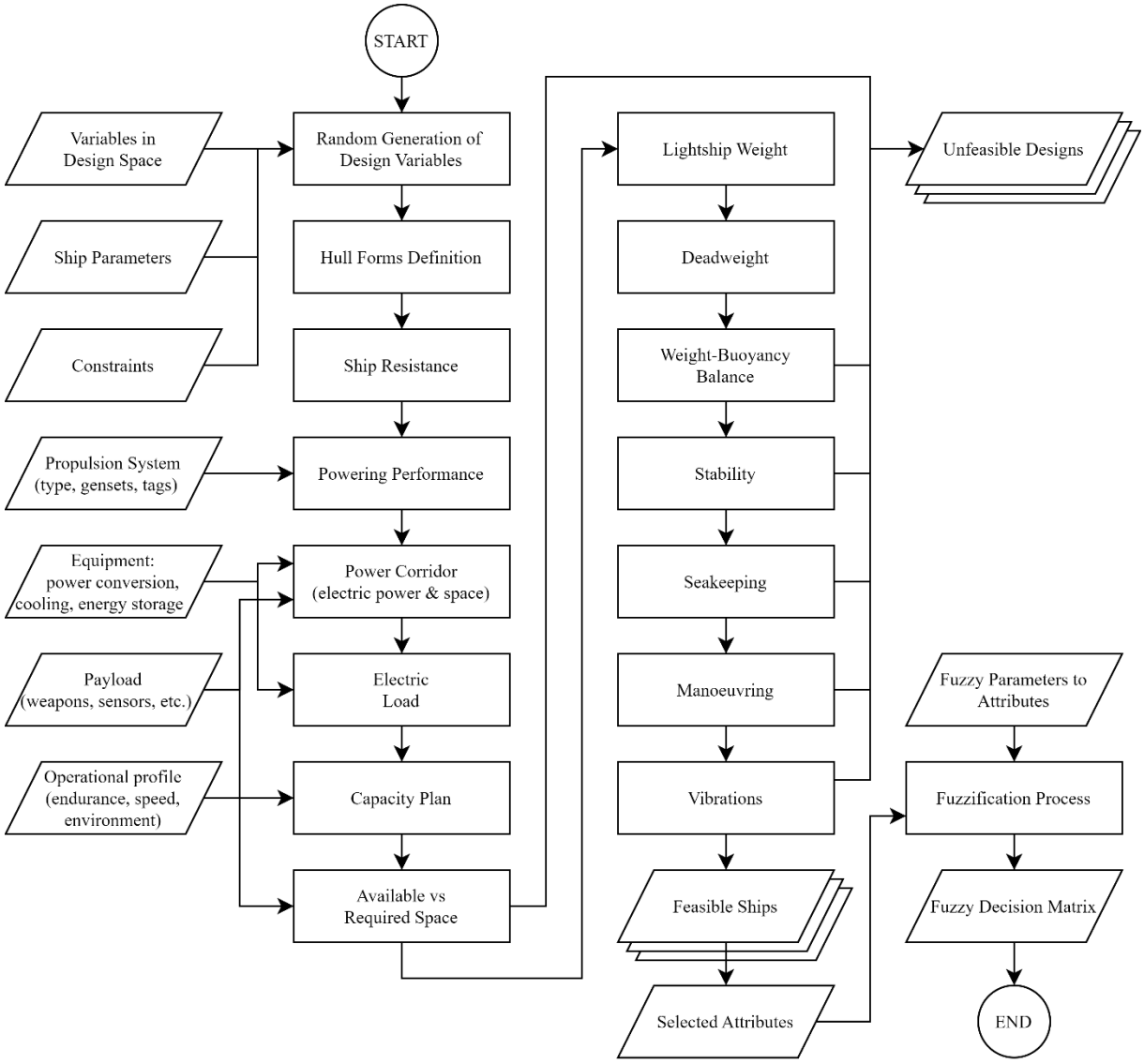

Figure 2: Flowchart of the mathematical design model

Ship Resistance

The still water resistance is evaluated by summing the bare hull resistance and the added resistance due to appendage as:

$$R_{CW} = R_{BH} + R_{APP} \quad [1]$$

Bare Hull Resistance. The resistance module estimates the resistance of the ship in calm water as well as in sea states 4, 5 and 6, at speeds ranging from 10 to 33 knots. Values of added resistance due to wind and hull roughness of 18 months are evaluated too.
The resistance in calm water is calculated following the DTMB methodology, where the residual resistance component is evaluated according to the algorithm of Fung (1991) that is statistically based on experimental measurements made on destroyer models with large transom sterns. The added resistance due to hull roughness and fouling is taken into account adding the allowance correlation according to formulas proposed by Townsin et al. (1981).

Appendage Resistance. A set of empirical formulas (Kirkman et al., 1979) are used to calculate separately the added resistance of each appendage, such as bilge keels, propellers, rudders, and shaft lines. The area of the bilge keels is taken as 2.5% of the waterplane area at the design draft to make more effective their contribution to roll damping. The sonar dome is considered as a part of the hull so contributing to the frictional resistance component of the bare hull. Added resistance due to steering is estimated using approximate formulas given by Norrbin (1972).

Added Resistance due to Wind and Waves. The added resistance in an irregular sea is based on the superposition principle for the components of the wave, motion and resistance spectra as well as on the assumption of linearity for the ship response. In a wave spectrum, the mean added resistance in regular waves is then calculated from

$$\bar{R}_{AW} = 2 \int_0^\infty \frac{R_{AW}}{\zeta_a^2}(\omega_e) \cdot S_\zeta(\omega_e)\, d\omega_e \qquad [2]$$

where ζ_a is the wave amplitude, ω_e is the encounter frequency, S_ζ is the spectral value. R_{aw} is determined using the formulation of Lang and Mao (2020) in unidirectional head regular waves:

$$R_{AW} = \frac{1}{2}\rho g\, \zeta_a^2\, B\, B_f\, \alpha_T (1 + \alpha_V) \left(\frac{0.19}{C_B}\right) \left(\frac{\lambda}{L_{PP}}\right)^{Fn-1.11} \qquad [3]$$

where λ is the wave length, B_f is the bluntness coefficient of the design waterline, α_V is the speed correction factor depending on Froude number (Liu and Papanikolaou, 2016), and α_T is the draft correction factor (Kwon, 2008).
Calculations are performed at SS4, SS5 and SS6, which correspond to significant wave heights of 1.875, 3.250, and 5.000 meters according to the WMO. They account for a frequency of 43% in the North Atlantic.
The resistance due to wind is calculated for head wind as:

$$R_W = 0.5\, C_X\, \rho_a\, V_R^2\, A_T \qquad [4]$$

where $V_R = V_S + V_W$, ρ_a is the air density, and A_T is the transverse ship area esposed to wind. The wind resistance coefficient in the longitudinal direction, C_X, given by the Isherwood formula (1973). The wind speed is correlated to the significant wave height as follows:

$$V_W = 6.851\sqrt{H_{1/3}} \qquad [5]$$

Powering Performance

This module calculates the power developed at the speeds of interest in the required operating conditions, and determines the fuel consumption for each speed. The 'design point' of the fixed-pitch propeller is selected at the combat speed in a given sea state in order to take into account the increased loads the propeller will encounter over the years.
When a ship sails in a rough sea, the quasi-propulsive performance, η_D, decreases compared to calm water, since the open-water propeller efficiency decreases much more than the increase in hull efficiency. Minsaas et al. (1983) provided the following approximations for the reduction of thrust and torque coefficient because of lower propeller submergence due to waves and ship motions:

$$K_{T_\beta} = \beta \cdot K_T \qquad K_{Q_\beta} = \beta^{0.8} \cdot K_Q \qquad [6]$$

where $= 1 - 0.675[1 - 0.769\, h/R]^{1.258}$ for $h/R < 1.3$, while the hull efficiency increases slightly due to the increase in the wake fraction and the irrelevant variation of the thrust deduction factor.
Change in the effective wake fraction due to hull roughness is estimated by applying a modified version of ITTC-1978 formula for full-scale wake prediction. Losses in propeller efficiency due to roughness and fouling are evaluated as proposed by Townsin (1983).

Power Corridor

In DESMAD, the power corridor keeps its width and height constant for each generated ship, whereas its length varies depending on the ship length and its subdivision. These values dictate the allocation of dedicated volumes and areas for each design alternative within the required space module. By determining the total power requirements for payload, propulsion, and other non-vital loads through the Electric Load and Powering Performance modules, the volume required by all modules positioned in the power corridor can be assessed. Assuming a standard-sized cabinet within the power corridor (1.60 m wide, 2 m high) and employing a volume-to-power conversion for all main components, the occupied length in the power corridor can be calculated and compared to the available length. In this way, non-feasible solutions can be excluded and free length in

the power corridor reserved for future upgrades can be assessed. If a zonal distribution system is implemented, the available, required and free lengths are defined zone by zone to ensure proper accommodation of all components.

Electric Load

The electrical load module assesses the maximum electric load in the winter cruise condition, including margins, since it is associated with the highest fuel consumption. The electric power value is obtained from the gensets, where a factor 0.91 is introduced to transform mechanical power into electrical power. The latter is the sum of payload electric power and non-payload functional electric load, including auxiliaries, outfitting, crew accommodations, heating, ventilation, and air conditioning (HVAC). In particular, the HVAC electric load power value is a function of the net volume of the ship, which is calculated by subtracting from the total volume of hull and superstructures the volumes of the engine and auxiliary rooms, the fuel tanks, the fore and aft peaks, the lavender water and grey water tanks, the trunks for aspiration and exhausted gas, as well as the volumes occupied by the military system. The payload electric load is considered an input, whose power value is determined by summing all the electric loads that are required to be installed onboard for performing the ship-specific missions (e.g., weapon systems, sensors, etc.). The non-payload electric load is automatically evaluated based on the ship's propulsion and manoeuvring performance, the number of crew members, and so on. All formulas introduced in this module are empirical. A margin is added to compensate for voltage fluctuations.

Capacity Plan

To assess the required volume of tanks, first the fuel consumption required for the generators shall be assessed. Since it is the sum of the propulsion and electric consumptions, it turns out to vary significantly with different speeds, with the electric load associated with each operating condition, and with the demand of the military equipment (weapons, sensors, cooling).
In this respect, we deem that at the concept design level it is useless to try to make the gensets operate at the optimal load, i.e. the one with the lowest consumption. This strategy has the advantage of ensuring that the range constraint at cruising speed is respected with a safe margin. The fuel amount for the gas turbines is the same for all designs, whilst for the gensets the fuel rate is a function of the delivered power for the low, cruise and endurance speed, and of the power demand not satisfied by the gas turbines at combat and top speeds.
Fuel tanks must have sufficient volume to guarantee the range required at endurance speed. Other tanks are needed for lubrication oil, fresh water, ballast water, sewage, waste oil, and helicopter fuel. The volume of these tanks is calculated by means of simple empirical formulas.

Available vs Required Space

The space balance of a ship has an overriding importance on the overall ship's effectiveness. Arrangement of spaces in the general arrangement plan is evaluated concurrently with hullform selection. Design whose available spaces (areas and volumes) are lower than required, are discarded immediately.
The subdivision scheme considers constraints on the location of machinery spaces, the need to have a discrete number of subdivisions of at least minimum length, as well as safety considerations. Subdivision arrangement and compartment arrangement follow the requirements of RINAMIL (2017a). The Available vs Required Space module evaluates available space within the hull against power corridor volume, machinery arrangement and tankage requirements based on length, height, and volume of machinery spaces for the required propulsion plant and auxiliary machinery. Tankage volume is validated against the required endurance fuel. Available ship areas and volumes are calculated for payload items and a variety of ship functional purposes. The superstructure and deckhouse above the main deck are specifically sized to meet design requirements for the remainder of the required payload, crew, and ship functions.

Lightship Weight

The destroyer employs an all-steel construction. The components of the lightship weight (LSW) are classified by the US Navy Ship Work Breakdown System (SWBS). LSW is divided into six main groups, consisting of groups 100 through 600. Assessment of the hull steel weight (group 100) requires an iterative process since the weight of foundations can be determined only after having calculated the weight of the groups from 200 to 600, with due accuracy for 200-machinery group, 300-electric plant and 500-auxiliaries. A weight margin factor of 7.5 percent is added to the computed LSW; it includes 2.5% for future growth.
The longitudinal centre of gravity is assumed to coincide with LCB, whilst KG is increased with a margin of 3 percent.
The hull structure is divided into three primary components: longitudinal structures, transverse structures and super-structures. The weight of each component is calculated using the metamodels obtained from the statistical analysis of the results obtained from the structural calculations on the hundred ships in the database. All other weights in LSW are evaluated using empirical formulas as a function of the ship’s main dimensions and coefficients.

Deadweight

The deadweight (DWT) is the sum of the consumables (fuel weight, lubrication oil weight) and payload. It also includes the ballast water for trim adjustment through a compensation system.
The payload is mostly determined by the military payload in Group 400 and the entire Group 700, which consists of a fixed payload and a variable payload. The latter includes weights of the crew, provisions and required stores, which depends on the crew size and the required stores period, as well as on the helicopters, JP-5 fuel, missiles and ammunition. The fixed payload is basically the combat system weight (vertical launch system, railgun, weapons handling, etc.).

Weight-Buoyancy Balance

The balance between the ship buoyancy and ship weight is assured through applying a crisp constraint. In detail, the relative difference between full load displacement Δ_{FL} and the total ship weight W_{FL} shall be within 2.5 percent. This condition is stated as:

$$\frac{|\Delta_{FL} - W_{FL}|}{\Delta_{FL}} \leq 0.025 \quad [7]$$

Stability

The general intact stability criteria of naval ships (RINA, 2017b) to be fulfilled for the righting lever curve are more stringent than the IMO criteria for merchant ships. Intact stability criteria are verified using empirical formulas for calculating cross curves of stability, as outlined by Degan et al. (2021). Subsequently, the righting lever curve is evaluated at the design draft to ensure compliance with stability criteria. A further criterion for intact stability is the feasibility range of the ratio $C_{GM/B}$ between the metacentric height GM and ship beam at the design waterline B_{WL}. According to values assumed for the DDGx ship model, it can be expressed as:

$$0.090 \leq C_{GM/B} \leq 0.135 \quad [8]$$

Damage stability compliance is evaluated by determining the geometric floodable length using regression equations, following the approach of Mauro et al. (2019). These floodable lengths are then utilized to guide bulkhead allocation, as described by Braidotti & Prpić-Oršić (2023).

Seakeeping

First of all, the module calculates the natural periods of heave, pitch and roll, subject to two crisp constraints: i) the natural roll period must be higher than 10 seconds; ii) the double heave and pitch periods must be quite different from the roll period.
For seakeeping assessment, various tools are available such as linear numerical codes based on "strip theory", completely reliable for single-hull ships up to Froude numbers equal to 0.35, nonlinear numerical codes, experimental tests on physical models and nonlinear numerical simulations. As stated above, the strategy underlying the concept design does not involve any direct calculation. Therefore, several metamodels were built at the University of Trieste (UT) where many ship responses were evaluated for the hundred ships generated with the DoE. Calculations were performed for the annual average significant wave height in the North Atlantic ($H_{1/3} \approx 2.450$ m) at endurance speed. The sea was described by the two-parameter Bretschneider spectrum. The metamodels refer only to the root-mean-square (RMS) of motions and effects induced in the vertical plane in head sea. This hypothesis is entirely consistent with what was stated by Bales (1980): “It was further assumed that both the index and the relationship could be adequately quantified using analytically-based results for long-crested, head seas. The implications of this assumption are that rolling motion can be adequately controlled by subsequent appendage design, and that coupling effects from the lateral modes at oblique relative headings and/or in short-crested seas will not significantly alter trend identified under the relatively simple conditions evaluated”.
The valued responses are heave, pitch, vertical acceleration at the bridge, relative motion and relative velocity at the propeller tip at 12 o’clock, relative motion at helideck, relative motion at sonar dome, vertical acceleration at railgun foundation, slamming and deck wetness. Corresponding metamodels may be expressed in functional terms as:

$$MS = f\left(\frac{BM_L}{L}, \frac{L}{B}, \frac{L}{T}, \frac{B_{tr}}{T}, \frac{LCB - LCF}{T}, C_{WP}, C_{VP}\right) \quad [9]$$

The operability limits for naval ships are given in Table 1. The more stringent ones are selected as crisp criteria in the mathematical design model. The RMS responses of the metamodels are unified in the seakeeping measure of performance (MOP) after weighing each seakeeping characteristic using the AHP method (Saaty, 1980).

Table 1. Seakeeping criteria

Recommended and Default Criteria	NATO STANAG (2020)	NORDFORSK (1987)	RINA (2017c)
Pitch (RMS)	1.5 deg		
Vertical acceleration at bridge (RMS)	2.0 m/s2	2.75 m/s2	
Motion sickness incidence (MSI)	20% in 4 hrs		35% in 2 hrs
Slamming		3% probability	20/hr
Deck wetness		5% probability	30/hr
Propeller emergence			90/hr

Manoeuvring

As with the other properties of the destroyer, in the ship concept design a quick computation is required to assess the ship's maneuverability. This module predicts the attributes of course keeping, advance and turning ability, quantified by the tactical diameter, using the metamodels built on the basis of results obtained by calculations on ships of the destroyers' database, carried out with a code (Nabergoj, 2000) made available to UNITS. The code integrates the manoeuvring nonlinear equations by means of a fourth-order, variable step Runge-Kutta method. It uses hydrodynamic derivatives calculated using the formulas of Yoshimura and Masumoto (2011). The manoeuvring model is applied only in calm water.
To evaluate the path keeping, the evolution index of Norrbin (1971) – the so-called P-number -is used.
Maneuverability criteria for merchant ships are generally not applicable to the special requirements of naval ships. The attributes are subject to rules established by RINA (2017c). A bounding value of 3.5 ship lengths is applied for a minimum tactical diameter, whereas the P-number is required to have a minimum value of 5.0.

Vibrations

The module calculates the first four natural frequencies of vertical hull vibration mode based on regression analysis of a large number of full-scale measurements, made available to UNITS. Then, the risk of unwanted resonance is estimated by comparing these hull natural frequencies with three excitation frequencies, i.e. engine second-order frequency, propeller imbalance and propeller blade frequency. An averting membership grade function is used to assign aspiration level to avoid the worst case of resonance between the excitation and hull natural frequency.

DESIGN OF THE BASELINE DESTROYER

Technical Specification

The technical specification is a more stringent variant than that formulated by the Italian Navy regarding the operating conditions. The military payload is that assumed for the USA Notional Ship (Chalfantet al., 2015; Chalfant 2017). The destroyer is required to operate in the wider Mediterranean Sea, the Arabian Gulf, and the Red Sea, as well as in the Atlantic, Indian and Pacific Oceans.
The ship must be capable of carrying out its functions for at least thirty years, in which operation must be guaranteed for at least 70% of the time, assuming as a reference employment away from national basins periods of up to 8 months (6 in the area and 2 for transfer). It must ensure compliance with MARPOL TIER III regulations, ensure transit of 1000 miles at a minimum speed of 12 kt and stay in port for 7 days in ECA zones.
The ship propulsion system shall be based on a conventional twin propeller/rudder solution, powered by electric motors, realizing an all-electric ship. The onboard gensets have to supply both propulsion and onboard loads, exploiting an integrated power system.
The crew is assumed to have 26 officers, 25 non-commissioned officers, 78 sergeants, 80 troops, plus 21 additional accommodations. The standard reference for living spaces on board, food storage and waste treatment is the SMM-100 regulations of the Italian Navy (Marina Militare Italiana).
The ship shall be characterized by logistical autonomy of at least 45 days and must be energy efficient neutral, e.g. green plus notation. It must be able to retain black and grey water on board for at least 7 days. Regarding military payload, the ship is required to include (Chalfant, 2017):

- 1 x railgun (impulse of 10 MW)
- 1 x laser gun
- 2 x 76/62 naval gun
- 2 x machine guns close-in weapon system

- 2 x multipurpose rocket launcher
- 3 x fixed face radar in both S and X bands
- 2 x integrated topside array
- 2 x 48-cell Vertical Launching Systems (VLS)
- 1 x sonar in the bulbous bow

Power System Design

As the ship is all-electric, it is required to supply full power by means of electric generators, through a suitably sized integrated power system. The Power Corridor concept described above has been selected for this ship, and the Zonal Electric Power Distribution System (ZEDS) of Figure 3 has been defined. This solution offers significant advantages in terms of survivability and flexibility a ZEDS provides (Sulligoi et al., 2020) and is capable of managing large power level variations due to direct energy systems (Bosich et al., 2023), which are even more important for naval ships. The electrical zones follow the subdivision of the ship into Main Vertical Zones, and each can operate separately from the rest of the power system (provided that sufficient electrical power is available in the zone for the installed loads). Each load group is interfaced to one or both the power corridors by means of suitably sized power electronics converters, which have multiple functions. First, they step-down the voltage to the level required by the loads; second, they convert the DC voltage of the main buses in AC, if required by the loads; third, they manage the power flows in and out of the power corridors. Some of the loads (i.e., the chillers and the railgun) have no dedicated converter installed on the power corridor, because they either require specifically designed power supply systems (it is the case of the railgun), or they are supposed to already integrate conversion phases to perform their expected functions (it is the case of the chillers).
In relation to the onboard electric loads listed above, the definition of the interface converters' power has been made as follows:

- the 10 MW railgun requires a 17 MW power supply (Chalfant, 2017), which can be fully powered by either power corridor; the power supply is integrated into the railgun subsystems, thus interface converters are not required.
- the 300 kW laser requires a 0.5 MW interface converter, and can be fully powered by either power corridor.
- the 3 fixed-face radars in both S and X bands (3 MW total) and the integrated topside arrays (3 MW total) are powered by the same interface converters. The latter has a 4 MW size, thus being capable of supplying two-thirds of the total power from each power corridor. This is because contemporary and usage factors of these two loads are supposed to be not equal to one; despite this, full power operation is possible with both power corridors working and partial operation with half the power system down.
- the VLSs (0.5 MW for each set) are supposed to be fully operable also with one power corridor down, as well as the sonar in the bow (0.5 MW total), thus requiring equally sized interface converters on each side.
- the chillers, sized at 3.8 MW each to correctly manage all heat sources onboard and providing a 2 to 1 redundancy level, are fed alternatively by the two power corridors.
- other loads are also present onboard (e.g., the steering systems depicted in Figure 3, the cabin loads, and so on), which are alternatively supplied by the two power corridors through 2 MW interface converters. The latter are oversized by nearly 50%, to enable the supply of only the vital loads in the nearby zone in case of a fault (requiring a load shedding system to be put in place). This is highlighted by the dotted lines connecting such loads across zones in Figure 3.

The 80 MW all-electric propulsion system, which requires one 40 MW electric motor on each shaft, is designed to be capable of powering both the propellers (albeit at reduced power) with one power corridor down. To this aim, the electric motors are dual stator winding induction machines, where each winding can provide half of the power. The two windings are thus supplied by 20 MW converters, integrated into the power corridors (thus not located inside the engine rooms).
The electric power generation system (composed by two 22.7 MW gas turbines, two 16.3 MW diesel generators, and two 9.16 MW diesel generators) follows the same approach as the propulsion system, with dual stator winding machines providing half the power to each power corridor. This enables to deliver up to 48 MW of power to the ship loads also with one power corridor faulted. As can be seen in Figure 3, the power corridor is distributed in five zones. whose lengths are shown in Table 2.
Payload weight and volumes have been taken from (Chalfant, 2017), while the non-payload and the HVAC loads weights and volumes are calculated by the above-described mathematical model.
The Power Corridor main distribution, located in its bottom part (refer to Figure 1), operates in medium voltage, at 12 kV. It has been sized to transport up to 60 MW from one extremity to the other in each power corridor, providing a 25% margin with respect to the generators' power for future refitting. Different solutions can be used to deliver such power, here a busbar system has been selected, leading to a minimum required space of 44 cm in height and 15 in width, to which cooling, and power tap systems, must be added. Similarly, a weight of 50 kg/m must be considered for the busbars only, to which additional weight for power tap and enclosures must be added. To reduce the overall weight and volume of this element, a possible solution is to reduce its power sizing in the more external zones (i.e., zones 1 and 5), where only the power needed by the local loads is to be delivered. However, a full distribution sizing has been here used, to both enable the installation of more loads in these external zones and promote standardization of the power corridor components.
For what it concerns the power electronics converters installed in the power corridor, their weight and volume follow the values defined in Chalfant (2017), depicted in Table 5 for reference.

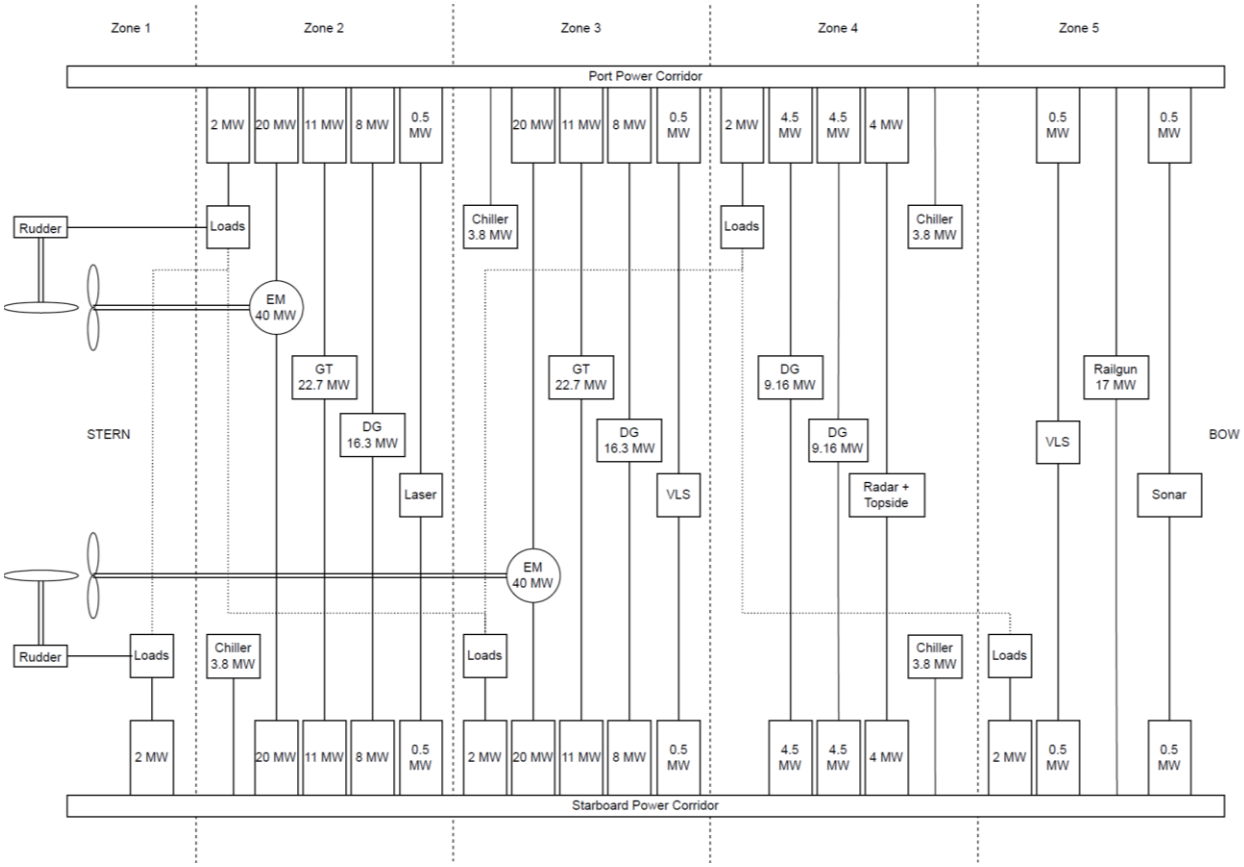

Figure 3: Zonal Electric Distribution System based on Power Corridor concept

Table 2: Available lengths of the zones

Zone	1	2	3	4	5
Length (m)	14.0	24.8	32.4	29.8	10.0

The overall Power Corridor sizing has a width of 1.6 m, which requires a total reserved space of 3.8 m on each ship side for ensuring correct accessibility for maintenance, and a converter rack height of 1.9 meters maximum, to be installed on top of a 0.6 m height distribution conduit (refer to Figure 1). The total length of the power corridor can be inferred from the ship GAP, while the single converters length has been evaluated as the one required to obtain the Table 3 volume, when the above-mentioned width and height are fixed.

Table 3: Nominal Power Converter Sizing Chart

Power Rating (MW)	1	2	3	4	6	8	10	12	14	18	22	24
Weight (t)	2.55	2.73	2.91	3.09	3.72	3.78	3.90	3.96	5.61	5.73	6.44	6.62
Volume (m^3)	12.9	12.9	12.9	12.9	15.1	15.1	15.1	15.1	20.8	20.8	24.2	24.2

Preliminary Design

The concept of the prototype design is that of a multi-mission ship whose combat system is fundamentally based on that of the Notional Ship (Chalfant, 2017). It is an all-electric twin-screw and two-rudder destroyer with a “tumblehome” hull form to reduce radar signature. It has a wide flaring bow, which significantly allows high speed in heavy sea conditions. A representative rendering of the ship model is shown in Figure 4 with its main characteristics listed in Table 4.
The main data of the individual fixed-pitch propeller and rudder is listed in Table 5. The propellers are designed based on the hydrodynamic load present in the battle scenario.
The operating profile is assumed on an annual basis and is given in Table 6 in terms of the percentage of time during which the destroyer sails at speeds and related operative conditions given in Table 4.

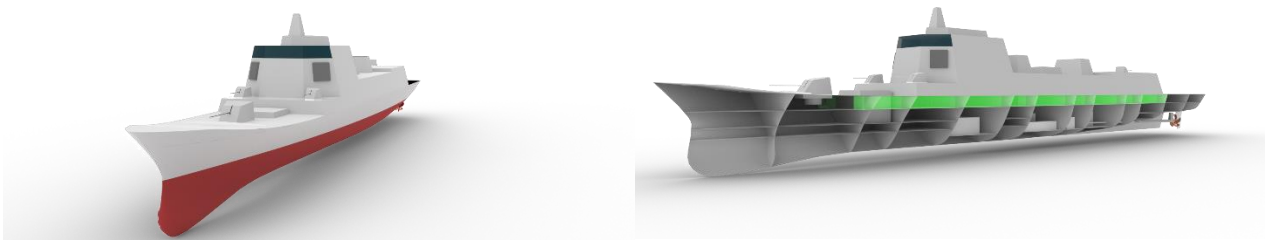

Figure 4: Rendering of the reference destroyer (in green: the port power corridor)

The total electrical power is obtained by adding the vital and non-vital electrical loads to the electrical demand requested by the sensors, weapons and chillers. It is worth noticing that the total power installed on board (95,780 kW) is more than 15,000 kW in excess of the maximum power required at a speed of 31 knots in sea state 4, in anticipation of an increase in power to be installed in the power runner in the future. For powering the full electric propulsion system at low and medium speed, it is sufficient to operate only the Diesel gensets (the size of the running ones depends on the speed, as shown in Table 6), while at peak and combat speed the ship operates with all the Diesel and the Gas Turbine gensets running. Finally, the MCR percentages of the gensets are reported for each speed. The values of baseline ship's attributes are given below in section "Ranking for the Best Compromise Design".

Table 4: General characteristics of the baseline ship

Length overall	L_{OA} = 179.000 m	Range at endurance speed	8000 nm
Length between perpendiculars	L_{PP} = 170.500 m	Low speed	12 kn @ SS6 + wind
Length at waterline	L_{WL} = 170.500 m	Cruise speed	18 kn @ SS5 + wind
Beam, maximum	B_{max} = 24.180 m	Endurance speed	20 kn @ SS5 +wind
Beam at design draft	B_{WL} = 22.250 m	Battle speed	28 kn @ SS4 + wind
Draft	T = 6.520 m	Top speed	31 kn @ SS4 + wind
Displacement	Δ = 12592 t	Complement	209
Longitudinal center of buoyancy	LCB = 84.24 m	Engines	2 x 9160 kW gensets
Longitudinal prismatic coefficient	C_P = 0.614		2 x 16030 kW gensets
Waterplane area coefficient	C_{WP} = 0.732		2 x 22700 kW tags
Vertical prismatic coefficient	C_{VP} = 0.675	Sensors, weapons, cooling	see Chalfant (2017)
Metacentric height	KM = 11.024 m	system, power conversion	
Vertical center of gravity	KG = 8.684 m	& distribution equipment	

Table 5: Propeller and rudder characteristics

Propeller		*Rudder*	
Diameter	= 4.620 m	Area	= 17.620 m^2
Pitch ratio	= 1.257	Span	= 4.895 m
Expanded rea ratio	= 0.986	Tip chord	= 3.600 m
Number of blades	= 5		

Table 6: Powering Performance

Ship Speed	V_S = 12 kn	V_S = 18 kn	V_S = 20 kn	V_S = 28 kn	V_S = 31 kn
Operating Time	10.0%	52.5%	30.0%	2.5%	5.0%
Delivered Power	P_D = 9592 kW	P_D = 12968 kW	P_D = 17852 kW	P_B = 39055 kW	P_B = 70855 kW
Total Electric Power	P_{EL} = 14726 kW	P_{EL} = 19796 kW	P_{EL} = 25164 kW	P_{EL} = 75415 kW	P_{EL} = 79740 kW
Fuel Consumption	2.701 t/h	3.636 t/h	4.622 t/h	5.752 t/h	6.518 t/h
Main Engines	Wärtsilä 8L46	Wärtsilä 14V46	Wärtsilä 14V46	LM 2500 + Wärtsilä 8V46 + Wärtsilä 14V46	LM 2500 + Wärtsilä 8V46 + Wärtsilä 14V46
Cont. Service Rating	80.6% MCR	61.9% MCR	78.6% MCR	35.6% MCR	58.7% MCR

FUZZIFIED DECISION SUPPORT SYSTEM

In the multiattribute design process, a large number of feasible designs is created by execution of the mathematical design model with a set of design variables generated by an adaptive Monte Carlo method. Constraints of min-max, crisp or fuzzy type may be applied to any attribute value generated within the MDM. A design is feasible if all attributes are within the given limits. Among all feasible designs, only non-dominated ones in the Pareto sense are retained. The product is a hypersurface of non-dominated designs subject to a final selection strategy.

Membership Grade Function

Ship design is a decision-making process whose nature generally involves uncertainty, vagueness or imprecision in the design attributes and constraints. Some of them are hard, i.e. based on physical laws or statutory norms, whereas some may be soft, i.e. based on the design team's aspiration level with uncertainty included. Moreover, in modeling the concept design process, deterministic algorithms are implemented to predict the attributes' values, which often cannot be determined exactly due to vagueness of many parameters and limited reliability of prediction methods. That is why the decision making necessitates a fuzzified decision support system. In fact, the concept design is intrinsically a fuzzy-logic problem where attributes may be weighed by the degree of membership reflecting the design team's knowledge and experience with the specific ship type.
To present the notion that an attribute is a member of a set A (for example, the RINA weather criterion rules) either fully or not at all, the function μ is introduced in Boolean terms as:

$$\mu_A(x) = \begin{cases} 1 & \text{if and only if} \quad x \in A \\ 0 & \text{if and only if} \quad x \notin A \end{cases} \qquad [10]$$

stating that the design x has either a 0 or a 1 membership grade in the given set. When $\mu_A(x)$ contains only the two points 0 and 1, the set A is non-fuzzy (crisp); in the above example, the weather criterion determines whether design x is feasible or unfeasible.
The i^{th} attribute's scores of a feasible design are viewed as a fuzzy set A, defined as the ordered set of pairs:

$$\{x_i, \mu_A(x_i)\} \qquad i = 1, 2, \dots, n \qquad [11]$$

where x_i denotes a design in the fuzzy set, whereas $\mu_A(x_i)$ represents the degree of truth, i.e. the membership grade function $0 \leq \mu_A(x_i) \leq 1$ for any $x \in A$
The mathematical theory of fuzzy sets (Zadeh, 1965), also referred to as fuzzy logic, is concerned with the aspiration level $\mu_A(x)$ reached by the outcome of an attribute, hence of a design.
Fuzzy sets may be treated as a collection of crisp sets by using the concept of an α-cut. An α-cut determines the crisp set A_α having all elements of A with a membership grade greater than α:

$$A_\alpha = \{x \in A \mid \mu_A(x) > 0\} \qquad [12]$$

Thus, α-cut sets correspond to discarding those elements of a fuzzy set that are 'extreme' in the sense of having 'low' membership grade in the set.
Among the three most important operations on any fuzzy sets, e.g. complement, union and intersection, the latter is the one useful in the MADM decision-making process. According to the intersection operation, the membership grade value of design x_i belonging to set A_1 and to set A_2 cannot be greater than the minimum of the two membership grade values:

$$\mu_{A_1 \cap A_2}(x_i) = \min\left[\mu_{A_1}(x), \mu_{A_2}(x_i)\right] \qquad [13]$$

Generalizing for n attributes, we can write for the degree of total membership grade $\mu_{\tilde{A}_j}$ of design x_i:

$$\mu_{\tilde{A}_j}(x_i) = \min\left[\mu_{A_1}(x_i), \dots, \mu_{A_k}(x_i), \dots, \mu_{A_n}(x_i)\right] \qquad j = 1, \dots, k, \dots, n \qquad [14]$$

Fuzzy MADM Selection

After generating a number of projects that adequately fill the design space, a fuzzy multiattribute decision-making method was implemented to identify the non-dominated designs and select the optimal vector of design attributes, e.g. the ideal design. It consists of six steps:

1. structuring the decision matrix;

2. determining the membership grade $\mu(x_i)$ for each attribute;
3. establishing the relative importance of the attributes by pairwise comparison;
4. weighing the degrees of attribute attainment $\mu(x_i)$ by the respective w_j so creating the intra-attribute fuzzy sets $\tilde{A}_j$;
5. finding the fuzzy set $\widetilde{D}$ of the non-dominated designs and the ideal design x_i^*;
6. selecting the preferred design x_i that has the minimum distance from $\widetilde{D}$ as the preferred design.

Decision Matrix. The decision matrix organizes the data available to the decision maker at the beginning of the selection process. A design problem with a total of m feasible designs described by n attributes is structured in a $m\ x\ n$ matrix $\tilde{A}$. Each element a_{ij} of the matrix is the performance rating of the design A_i with respect to attribute x_j.
The decision matrix should include only those attributes which vary significantly among the alternative designs and for which the design team considers this variation significant.

Intra-Attribute Preference and Attribute Normalization. Intra-attribute preference reflects the objective importance of the different values of the same attribute according to the maximum target the design team aspires to. Although different approaches look alike (e.g. value function concept), the membership grade approach from the fuzzy set theory is considered the most suitable tool for the purpose (Kosko, 1994). Among different formulations of membership grade functions developed so far, the generalization of Nehrling's function (Nehrling, 1985) is introduced in this study. Four types are defined, i.e. attracting, ascending, descending, and averting, whose formulation is provided in Table 7.

Table 7: Formulation of membership grade functions

Attracting	$\mu(x_i) = \dfrac{1}{1 + \left\lvert\dfrac{x_1 - x_i}{d}\right\rvert^N}$	*Averting*	$\mu(x_i) = 1 - \dfrac{1}{1 + \left\lvert\dfrac{x_1 - x_i}{d}\right\rvert^N}$
Ascending	for $x_i < x_1$ $\quad \mu(x_i) = \dfrac{1}{1 + \left\lvert\dfrac{x_1 - x_i}{d}\right\rvert^N}$ for $x_i \geq x_1$ $\quad \mu(x_i) = 1$	*Descending*	for $x_i \leq x_1$ $\quad \mu(x_i) = 1$ for $x_i > x_1$ $\quad \mu(x_i) = \dfrac{1}{1 + \left\lvert\dfrac{x_1 - x_i}{d}\right\rvert^N}$

Two points on the membership grade curve are important and may be defined as
$x = x_1$ the level of an attribute that is 100% satisfactory - $\mu(x) = 1$ -, i.e. the level that may be expected to be reached by the best design with respect to the specific attribute;
$x = x_1 \pm d$ the level that is only 50% percent satisfactory - $\mu(x) = 0.5$ -, where d is the variation imposed subjectively by the decision maker compared to the aspiration level.
Selecting the proper type and assigning appropriate values to d and N (2, 4, 6, 8), the design team may shape the membership function for each attribute.

Inter-Attribute preference. Design attribute values serve as a basis for selection of the final design among all non-dominated designs. As the attributes are not equally influential, in order to reflect their relative importance it is necessary to weigh them. One solution is to obtain a weighted membership grade by multiplication with a weighting factor reflecting the subjective preferences of the design team. In this respect, the Analytical Hierarchy Process (AHP) method, which was pioneered and developed by Saaty (1980), converts subjective assessments of relative importance to a set of weights. It provides a useful mechanism for checking the consistency of the evaluation measures for attributes generated by the mathematical design model.

Weighing the Intra-Attribute Fuzzy Sets. According to Nehrling (1985), weights were originally applied to membership grade as:

$$\left[\mu_j(x_i)\right]^{w_j} = \frac{\mu_j(x_i)}{1 + w_i} \qquad [15]$$

which did not take into account the number of attributes n.
To obtain better resolution of small weights when $n > 5$, a better solution was derived by Grubišić et al. (1997, 1998) as:

$$\left[\mu_j(x_i)\right]^{w_j} = \frac{\mu_j(x_i)}{1 + n\ (w_i - w_{min})} \qquad [16]$$

Hence, membership grades are multiplied by 1 for $w_i = w_{min}$ and by values progressively smaller than 1 for other weights.

Choice of the Preferred Design. Among a large set of feasible designs, no dominant design will exist that is better than all other designs in terms of all attributes. At the same time, it is impossible to minimize/maximize all attributes simultaneously. Since good values of some attributes inevitably go with poor values of others, the goal of the MADM method is to find the 'best compromise' solution following the concept introduced by Zeleny (1982). It can be obtained from a set of design alternatives referred to as the Pareto frontier, which consists of designs having a simple and desirable property, i.e. dominance (Pareto, 1906). According to this strong normative statement, a design is non-dominated, denoted as ND, when no attribute can be further improved without causing at least one of the other attributes to decline. Non-dominance can be expressed in terms of a simple vector comparison. If $x^j = \left(x_1^j, x_2^j, \dots, x_n^j\right)$ and $x^k = (x_1^k, x_2^k, \dots, x_n^k)$ are two designs of n attributes x^j dominates x^k if $x_i^j \geq x_i^k$ and $x_i^j > x_i^k$ for at least one attribute i and thus design x^k is discarded. Further pairwise comparison between feasible alternatives creates a set of non-dominated designs. At the same time, the collection of the highest achievable membership grades (attribute maxima) with all considered attributes form a composite, an ideal design x^* or 'utopia point' (Yu, 1973), denoted as $x^* = (x_1^*, x_2^*, \dots, x_n^*)$.
The hypersurface of the non-dominated designs defines the boundary of the production possibility, e.g. the limits attainable with each primary attribute depending on constraints of technological (and economic) nature. Then for each non-dominated design a fuzzy set $\tilde{A}$ in X is the set of ordered pairs:

$$\tilde{A}_j = \left\{x_i, \left[\mu_j(x_i)\right]^{w_j}, \quad x_i \in X\right\} \qquad [17]$$

The intersection of all $\tilde{A}_j$ forms the fuzzy decision set $\tilde{D}$ represented by the membership function $\mu_D(x_i)$ which describes the 'utopia point'.
The final step is to identify the 'best compromise' design from those contained in the fuzzy decision set $\tilde{D}$ represented by the membership function $\mu_D(x_i)$. As the rationale of the designers' choice is to prefer the solutions that are closer to the 'ideal design', the 'best compromise' design is that one with the minimum distance to the ideal design. In a fuzzy environment, the degree of closeness to the anchor value is measured via the Čebyšev metric as follows:

$$L_\infty = \min_j \left\{1 - \min_i \left[\mu_j(x_i)\right]_{i=1,n}^{w_j}\right\}_{j=1,ND} \qquad [18]$$

where the distance parameter ∞ means that the maximum possible weight is given to the largest deviation according to Equation [16].

MADM SELECTION PROCESS

The goal of the decision model is to simulate the decision-making of the design team in selecting the 'best compromise' destroyer from the Pareto frontier. The selection process is modelled as a MADM problem. The overall process for generating feasible designs, filtering non-dominated designs and selecting the preferred solution flows through the following steps: (i) identification of design variables, parameters, attributes and definition of individual min-max design space; (ii) generation of feasible design via an adaptive Monte Carlo method; (iii) definition of intra-attribute fuzzy functions and interactive inter-attribute preference; (iv) structuring the non-dominated design hypersurface; (v) selection of the 'best compromise' design.

Generation of Feasible Designs. The implemented mathematical design model is applied to the concept design of a class of destroyers whose main novelty is the presence of the power corridor. The propulsion system, the power from the electrical generators, the crew size, the vital and non-vital loads, the weapons and ammunition, the sensors, and the conversion and equipment distribution system are the same for all candidate designs. Viable and feasible solutions were generated subject to crisp constraints and soft constraints treated as attributes.

Variables, Parameters, Attributes and Constraints. The generated designs are uniquely defined by six independent variables given in Table 8, which define the design space through min-max values.

Table 8: Initial design space

Variable	L_{PP}/B_{WL}	B_{WL}/T	L_{PP}/T	C_P	C_{VP}	$L_{WL}/\nabla^{1/3}$
Minimal Value	7.250	3.000	23.750	0.615	0.600	7.000
Maximal Value	8.000	3.750	27.250	0.675	0.700	7.750

All candidate ships have data that is held fixed in a generation run, such as deck heights, number of zones, gas turbines, gensets, weapons, sensors, radars, cooling equipment, power conversion and equipment data, power corridor size, etc. The geometric topology and equipment are determined in advance as a result of the initial design of a destroyer prototype, which can be considered as the guess value to activate the mathematical design model.
Note that only the hull is defined by the random generation and not the superstructure. The size of the superstructure and deckhouse is a function of the length and beam of the hull. Not all generated ships yield feasible solutions since many other geometrical constraints are introduced which implicitly further restrict the multidimensional design space. The primary min-max constraints, which further restrict the design space, are illustrated in Table 9.
The mathematical design model calculates the primary and secondary attributes of feasible designs given in Table 10 together with their codes to simplify the writing of subsequent tables.
Attributes Y5 and Y10 are given as grades to reduce the number of attributes. Due importance is assigned to seakeeping and manoeuvring attributes because they heavily influence the operability of the ship.

Table 9: Geometrical constraints

Parameter	C_B	B_{ML}/L_{PP}	KB/B	Δ [t]	B_{MAX} [m]	$L_{WL}/\nabla^{1/3}$	i_E [deg]
Minimal Value	0.450	2.015	0.150	12250	23.750	7.000	5
Maximal Value	0.525	2.925	0.205	13000	25.250	7.750	10

Table 10: Attributes in the design process

Primary Attribute	Code	Secondary Attributes	Code
Fuel consumption at endurance speed (t/h)	Y1	Tankage volume (m3)	Y11
Power coefficient (-)	Y2	Metacenter height-to-beam ratio (-)	Y12
Weight-buoyancy balance (-)	Y3	Delivered power at endurance speed (kW)	Y13
Maximum speed (kn)	Y4	Delivered power at top speed (kW)	Y14
MOP membership grade function (-)	Y5	Electric load (kW)	Y15
Tactical diameter-to-length ratio (-)	Y6	Non-vital payload electric load (kW)	Y16
P-number (-)	Y7	HVAC electric load (kW)	Y17
Payload fraction (-)	Y8	Pitch (deg)	Y18
Available length for extra power corridor (m)	Y9	Volume of engine rooms (m3)	Y19
Vibration membership grade function (-)	Y10	Volume of power corridor (m3)	Y20

Outcomes of the Generation Process. The concept design starts with the generation of feasible designs. Fifty thousand destroyers were randomly generated. Only a little more than two thousand designs were found to be acceptable, overcoming all constraints. The cause of the unfeasibility of most of the ships was due to the fact that they had one or more geometric characteristics external to the design space. Other causes of elimination were, in decreasing order, an excessive detachment from the weight-thrust balance and non-compliance with the criteria of stability, seakeeping and manoeuvrability.
The process of design selection is interactive since designers might change and refine their preferences (sensitivity study). It is, therefore, of great importance to provide the design team with fast insight into multidimensional design and attribute spaces. To help in guiding the decision-making process a graphic support should be added.
For this purpose, three types of diagrams are proposed with the following combinations:

variable – variable	X-design space projection
variable – attribute	cross projection
attribute – attribute	Y-attribute space projection

The first group that relates the main dimensions and geometric coefficients to each other, serves to immediately identify the design space of feasible designs, so allowing to carry out an initial reduction of the feasible design space.
The second group is used to analyze the influence of any variable upon any attribute. It is useful for quantitatively predicting the effect of changing any variable on any attribute and for reducing the spans within which the variables are going to be generated in a next try. In this way, density of the non-dominated designs close to the ideal design may be increased.
The third group may be used as a guide to identify advantageous regions and to gain an impression of what may be the penalty for departing from the ideal solution.
Two examples in the X-design space are given in Figure 5. As can be seen, the feasible range of B/T ratio is dramatically reduced and reduces as the L/B ratio increases, making it unthinkable to have destroyers with L/B ratios tending towards 8. Relationship between C_B and C_{VP} allows to determine the feasible range for the waterline design coefficient, e.g. $0.685 \leq C_{WP} \leq 0.748$.

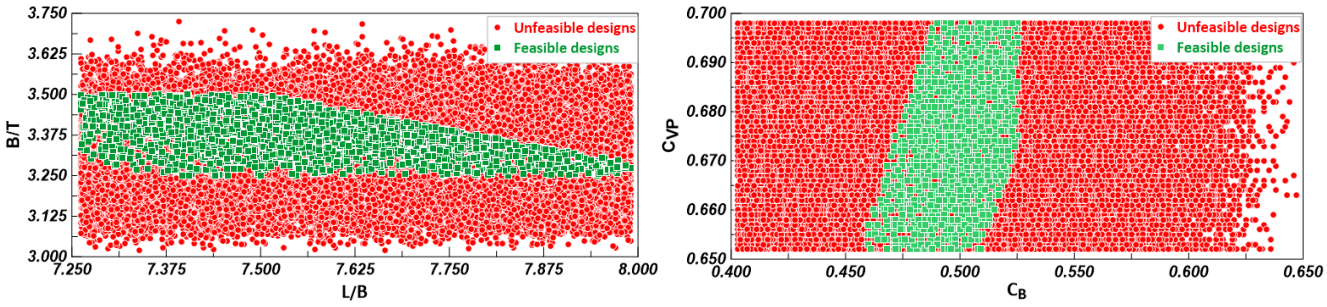

Figure 5: Variable-variable diagrams

Selecting the Preferred Designs

The purpose of the following analysis is to rate the overall performance of the feasible alternatives via the proper assignment of numerical grades to attributes and to rank the best designs.

Defining the Fuzzy Functions. The subjective decision on the aspiration level and relevance of each attribute is summarized in Table 11. A more stringent aspiration level (n = 2) is assigned to the hourly fuel consumption and free space in the power corridor for future storage of batteries.

Table 11: Selection of the membership grade functions

Attribute	Y1	Y2	Y3	Y4	Y5	Y6	Y7	Y8	Y9	Y10
Target	4.075	0.455	0	32.500	1.000	2.350	0.600	0.080	12.00	1.000
d	0.275	0.020	250	1.000	0.300	0.500	0.030	0.005	8.000	0.400
n	2	6	4	6	4	4	6	8	2	2
Fuzzy	Z-type	Z-type	Ω-type	S-type	Z-type	Z-type	S-type	S-type	S-type	U-type
α-cut	0.60	0.50	0.75	0.50	0.70	0.40	0.35	0.25	0.50	0.60

Non-dominated and Ideal Designs. The ideal solution (zenith) is characterized by the values of the attributes shown in Table 12, which represent the highest membership grades reached by different non-dominated designs in the multidimensional attribute space.

Table 12: Attributes of the Ideal Design

Fuel consumption	MDO = 4.025 t/h	Vertical acceleration at bridge	ACC_V = 1.466 m/s2
Power coefficient	C_{Power} = 8.08x10-2	Relative motion at helideck	RM_{hel} = 0.836 m
Maximum speed	V_{Max} = 32.44 kn	Nondimensional tactical diameter	D_{tac}/L = 2.526
Natural roll period	$T_{\emptyset}$ = 10.82 s	Available length for future power corridor	L_{PC} = 11.650 m

It is worth noting that the cross projections in Figure 6 show that both the baseline ship and ideal ship are very close to the Pareto frontier. Since both diagrams represent the power-speed relationship, this attests to the excellent quality of the resistance prediction in calm and confused seas and the design of the propulsion system.

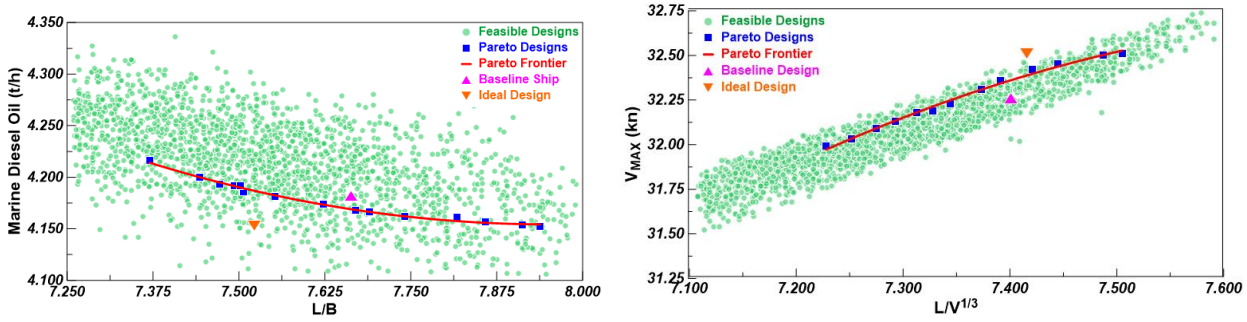

Figure 6: Variable–attribute graphs

Projection in the Y-space of the attribute-attribute relationship between available length for future enlargement of the power corridor and fuel consumption at endurance speed (left graph in Figure 7) shows that there are many possible designs with a longer power corridor than the baseline ship, but at the expense of a higher hourly rate.

Ranking for the Best Compromise Design. Measuring the distance of the non-dominated designs from the ideal point allowed us to build the ranking of the 'best possible' designs. Table 13 shows the comparison between the baseline ship and the 'best compromise' designs, where Design_1 and Design_3 are first and third in the ranking, respectively.

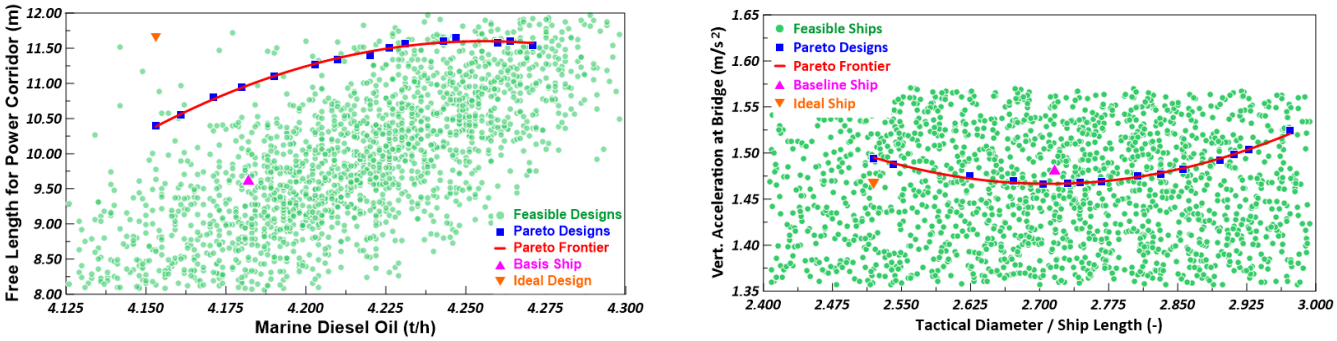

Figure 7: Attribute–attribute graphs

Table 13. Comparison between basic ship and the best possible designs

Item	*Baseline Ship*	*Design_1*	*Design_2*	*Design_3*
Main characteristics				
L_{OA}	179.00 m	180.18 m	181.75 m	180.52 m
L_{PP}	170.50 m	171.60 m	173.10 m	172.92 m
B_{MAX}	24.18 m	24.50 m	24.35 m	24.16 m
B_{WL}	22.25 m	22.52 m	22.40 m	22.18 m
T	6.52 m	6.37 m	6.48 m	6.56 m
Δ	12592 t	12500 t	12577 t	12413 t
C_P	0.612	0.613	0.606	0.604
C_{WP}	0.752	0.768	0.759	0.746
C_{VP}	0.656	0.629	0.649	0.642
KM	11.024 m	11.029 m	11.008 m	11.459 m
Primary attributes				
Y1	4.082 t/h	4.179 t/h	4.167 t/h	4.168 t/h
Y2	4.57 x 10-2	8.32 x 10-2	8.28 x 10-2	8.11 x 10-2
Y3	32.11 kn	32.03 kn	32.07 kn	32.04 kn
Y4	10.83 s	10.91 s	10.19 s	10.81 s
Y5	0.972	0.986	0.974	0.979
Y6	2.515	2.414	2.538	2.532
Y7	0.512	0.533	0.535	0.525
Y8	8.24 x 10-2	8.35 x 10-2	8.40 x 10-2	8.37 x 10-2
Y9	9.00 m	9.35 m	9.31 m	9.50 m
Y10	0.984	0.987	0.974	0.980
Secondary attributes				
Y11	3908 m3	3924 m3	3951 m3	3961 m3
Y12	0.109	0.110	0.106	0.122
Y13	19913 kW	20031 kW	20201 kW	20318 kW
Y14	74703 kW	74269 kW	76185 kW	75830 kW
Y15	3737 kW	3740 kW	3771 kW	3739 kW
Y16	1695 kW	1698 kW	1714 kW	1697 kW
Y17	1436 kW	1436 kW	1458 kW	1428 kW
Y18	1.145 deg	1.137 deg	1.125 deg	1.079 deg
Y19	3371 m3	3407 m3	3487 m3	3458 m3
Y20	2246 m3	2252 m3	2309 m3	2223 m3

Final Design Space. To conclude, one of the most important results of this study is that of having reduced the multidimensional design space, as shown in Table 14, where the initial design space is put in comparison with the final one as limited by the non-dominated designs.

Table 14. Design space before and after the concept design

Variable	L_{PP}/B_{WL}	B_{WL}/T	L_{PP}/T	C_P	C_{VP}	$L_{WL}/\nabla^{1/3}$
Initial Design Space						
Minimal Value	7.250	3.000	23.750	0.615	0.600	7.000
Maximal Value	8.000	3.750	27.250	0.675	0.700	7.750
Final Design Space						
Minimal Value	7.370	3.250	23.950	0.615	0.620	7.225
Maximal Value	7.920	3.500	23.720	0.675	0.675	7.5050

CONCLUSIONS

The contents of this paper are the result of a multidisciplinary cooperation project between MIT and UNITS, where the primary interest is to transfer know-how and technologies between still separated areas of naval architecture and electric-electronic engineering. We started from the belief that the introduction of advanced electrical and electronic technologies with integration of a power corridor requires a breakthrough in the design methodology (Sulligoi et al., 2016). To this purpose, a multiattribute decision-making process was applied to effectively select the 'best compromise' design which incorporates the power corridor. The results of the present work confirm the tendency towards increasing size of main surface combatants. It is about proposing ships that guarantee in the medium and long term the integration of additional systems and equipment that will absorb further electric and electronic power and require adequate space. It is for this reason that due importance has been given to the space available for future lengthening of the power corridor which is treated as a primary attribute in the decision-making process. Nevertheless, it has been here proved that in a main surface combatant, 2 power corridors, instead of original 4, might be sufficient to allocate all the required equipment with some margin.

The current MDM, although capable to provide reliable and interesting insights, can be further improved. Future enhancement of the mathematical model should include: (i) peak shaving to maximize the overall ship propulsive efficiency; (ii) competitive analysis of alternative power trains; (iii) optimization of power corridor layout; (iv) performance evaluation for energy storage systems to mitigate electric load fluctuations; (v) estimate of exhaust emissions by improvement of power distribution; and (vi) preliminary economic feasibility.

A limitation of this work is that all the primary and secondary attributes determined in the mathematical model are technical only. An economic module that calculates the annual average cost (AAC) index is completely missing. For a full picture of life-cycle costs, the economic module should include operating costs during the destroyer lifetime in addition to building costs including shipyard installation cost (excluding procurement cost) for command and armament. The AAC will be a dominant design criterion in a final analysis and selection of the 'best possible design'. This future activity requires knowledge of cost constraints.

CONTRIBUTION STATEMENT

Giorgio Trincas: Conceptualization, Methodology, Software, Investigation, Writing – Original Draft, Visualization, Project administration. **Luca Braidotti**: Conceptualization, Methodology, Software, Validation, Formal analysis, Resources, Data Curation, Writing – Original Draft, Visualization. **Andrea Vicenzutti**: Conceptualization, Validation, Formal analysis, Investigation, Data Curation, Writing – Original Draft, Visualization. **Andrea Alessia Tavagnutti**: Formal Analysis, Investigation. **Chathan M. Cooke**: Conceptualization, Investigation. **Julie Chalfant**: Conceptualization, Investigation, Writing – Review & Editing, Project Administration. **Vittorio Bucci**: Conceptualization, Investigation. **Chryssostomos Chryssostomidis**: Conceptualization, Investigation, Supervision. **Giorgio Sulligoi**: Conceptualization, Investigation, Resources, Writing – Review & Editing, Supervision, Funding acquisition.

ACKNOWLEDGEMENTS

Co-funded by the European Union, Horizon Europe Program - V-ACCESS Project; Grant agreement ID: 101096831. "Views and opinions expressed are however those of the authors only and do not necessarily reflect those of the European Union. Neither the European Union nor the granting authority can be held responsible for them".

This material is based upon research supported by, or in part by, the Office of Naval Research under award number ONR N00014-21-1-2124 Electric Ship Research and Development Consortium, by the National Oceanic and Atmospheric Administration (NOAA) under Grant Number NA22OAR4170126- MIT Sea Grant College Program, and by the Italian PNRM research projects “Naval Smart Grid (NaSG)” and "ETEF - Electric Test Facility".

REFERENCES

Andreasen, M.M. (1992). *The Theory od Domains*, Working Paper, Institute for Engineering Design, Technical University of Denmark, Lundby.

Bales, N.K. (1980). Optimizing the Seakeeping Performance of Destroyer-Type Hulls, 13th *Symposium on Naval Hydrodynamics*. Tokyo.

Bosich, D., Chiandone, M., Sulligoi, G., Tavagnutti, A. A., Vicenzutti, A. (2023). High-Performance Megawatt-Scale MVDC Zonal Electrical Distribution System Based on Power Electronics Open System Interfaces, *IEEE Transactions on Transportation Electrification*, 9(3), 4541-4551. DOI: 10.1109/TTE.2023.3244360

Braidotti, L., Prpić-Oršić, J. (2023). Bulkheads’ Position Optimisation in the Concept Design of Ships under Deterministic Rules, *Journal of Marine Science and Engineering*, 11(3), 546. DOI: https://doi.org/10.3390/jmse11030546.

Campana, E.F., Peri, D., Pinto, A, (2007), Multiobjective Optimization of a Containership Using Deterministic Particle Swarm Optimization, Journal of Ship Research, 51 (3), 217-228.

Chalfant, J. (2015). Early Stage Design for Electric Ship, *Proceedings of the IEEE on Electric Ship Technologies*, 103 (12), 2252-2266.

Chalfant, J., Ferrante, M. and Chryssostomidis, C. (2015). ‘Design of a Notional Ship for Use in the Development of Early-Stage Design Tools, *IEEE Electric Ship Technology Symposium* (ESTS), Alexandria, VA, 239-244.

Chalfant, J. (2017). ESRDC Notional Ship Data, *Electric Ship Research and Development Consortium*, Massachusetts Institute of Technology, Cambridge, available in https://esrdc.com/library/?q=node/762..

Cooke, M., Chryssostomidis, C. and Chalfant, J. (2017). Modular Integrated Power Corridor, *Proceedings of the 2017 IEEE Electric Ship Technologies Symposium* (ESTS), Arlington, VA, USA, 91-95

Cort, A. and Hills, W. (1987). Space Layout Design Using Computer Assisted Methods, *Naval Engineers Journal*, 249-260.

Degan, G., Braidotti, L., Marinò, A., Bucci, V. (2021). LCTC Ships Concept Design in the North Europe-Mediterranean Transport Scenario Focusing on Intact Stability Issues, *Journal of Marine Science and Engineering*, 9(3), 278. DOI: https://doi.org/10.3390/jmse9030278.

Derelöv, M. (2009). Identification of Potential Failure: On Evaluation of Conceptual Design, *Journal of Engineering Design*, 201-225.

Fung, S.C. (1991). Resistance and Powering Prediction for Transom Stern Hull Forms During Early Phase Ship Design, *Transactions SNAME*, 99, 29-84.

Grubišić, I., Zanić, V. and Trincas, G. (1997). Sensitivity of Multiattribute Design to Economic Environment: Shortsea Ro-Ro Vessels, *6th International Marine Design Conference, IMDC'97,* Newcastle upon Tyne, 201-216.

Grubišić, I., Zanić, V. and Bender, M. (1998). Fuzzy Attributes in Multi-Criterial Ship Concept Design Procedure, *International Design Conference - Design* ’98, Dubrovnik.

Hubka, V. and Eder, W.E. (19962). Design Science, Springer-Verlag, Berlin, ISBN 3-540-19997-7.,

Isherwood, R.M. (1973). Wind Resistance of Merchant Ships, *Transactions RINA*, 115, 327-338.

Kirkman, K.L., Sanders, D.G. and Slager, J.J. (1979). Methodology for Computation of Appendage Resistance, *NAVSEA*, Report 3213-79-40.

Kleijnen, J.P.C. (1987). *Statistical Tools for Simulation Practitioners*, Marcel Dekker, New York.

Kosko, B. (1994), *Fuzzy Thinking*, Flamingo, London.

Kwon, Y.J. (2008). Speed Loss due to Added Resistance in Wind and Waves, *The Naval Architect*, 14-16.

Lang, X. and Mao, W. (2020). A Semi-Empirical Model for Ship Speed Loss Prediction at Head Sea and Its Validation by Full-Scale Measurement”, *Ocean Engineering*, 209, 1-17.

Liu, S. and Papanikolaou, A. (2020). Regression Analysis of Experimental Data for Added Resistance in Waves of Arbitrary Heading and Development of a Semi-Empirical Formula, *Ocean Engineering*, 206, 1-17. doi.org/10.1016/ j.oceaneng.2020.107357.

Mauro, F., Braidotti, L., Trincas, G. (2019). A Model for Intact and Damage Stability Evaluation of CNG Ships during the Concept Design Stage, *Journal of Marine Science and Engineering*, 7(12), 750. DOI: https://doi.org/10.3390/jmse7120450.

Minsaas, L., Faltinsen, O.M. and Persson, B. (1983). On the Importance of Added Resistance, Propeller Immersion and and Propeller Ventilation for Large Ships in a Seaway, 2nd *International Symposium on Practical Design in Ship Building*, Tokyo & Seoul.

Myers, R.H. Montgomery, D.C. and Anderson-Cook C.M. (2016): *Response Surface Methodology*: *Process and Product Optimization Using Designed Experiments*, 3rd edition, Wiley, ISBN: 978-1-118-91601-8.

Nabergoj, R. (2020). Program MEDUSA, User's Guide, NASDIS PDS, Izola, Slovenia.
NATO (2000). Standardization Agreement (STANAG 4154). Common Procedures for Seakeeping in the Ship Design Process, NATO, *Military Agency for Standardization*.
Nehrling, B.C. (1985). Fuzzy Set Theory and General Arrangement Design, *Computer Applications in the Automation of Shipyard Operation and Ship Design, ICCAS 85*, Trieste, 319-328.
Norrbin, N.H. (1971). Theory and Observation on the Use of a Mathematical Model for Ship Manoeuvring in Deep and Confined Waters, 8th *Symposium in Naval Hydrodynamics*, Pasadena, California, 1971.
Norrbin, N.H. (1972). On the Added Resistance due to Steering on a Straight Course, *Proc. 13th ITTC*, Berlin & Hamburg.
NORDFORSK (1987). Assessment of Ship Performance in a Seaway, *The Nordic Co-operative Organization Project*: *Seakeeping Performance of Ships*, Copenhagen. ISBN 8798263714, 9788798263715, 1987.
Pahl, B., Beitz, W., Feldhusen, J. and Grote, K-H. (2007). *Engineering Design – A Systematic Approach*, Springer-Verlag, London, ISBN 978-1-84628-318-5.
Pareto, V. (1906). Handbook of Political Economics with an Introduction to the Social Science (in Italian), Società Editrice Libraria, Milan.
RINA (2017a). *RINAMIL, Rules for the Classification of Naval Ships*, Pt. B, Ch. 2, General Arrangement Design, 31-39.
RINA (2017b). *RINAMIL, Rules for the Classification of Naval Ships*, Pt. B, Ch. 3, General Arrangement Design, 47-55.
RINA (2017b). *RINAMIL, Rules for the Classification of Naval Ships*, Pt. B, Ch. 3, General Arrangement Design, 66-67.
Saaty, T.L. (1980). *The Analytical Hierarchy Process*: *Planning, Priority Setting, Resource Allocation*, McGraw Hill International, New York.
Sulligoi, G., Vicenzutti, A. and Menis, R. (2016). All-Electric Ship Design from Electrical Propulsion to Integrated Electrical and Electronic Power Systems, IEEE Transactions on Transportation and Electrification, 2(4), 507-521.
Sulligoi G., Bosich, D., Vicenzutti, A. and Khersonsky, Y. (2020). Design of Zonal Electrical Distribution Systems for Ships and Oil Platforms: Control Systems and Protections, *IEEE Transactions on Industry Applications*, 56 (5), 5656-5669, doi: 10.1109/TIA.2020.2999035.
Townsin, R.L. (1983). Bottom Condition and Fuel Conservation, VIII *WEGEMT Graduate School*, Gothenburg.
Townsin, R.L., Byrne, D., Svensen, T.E and Milne, A. (1981). Estimating the Technical and Economic Penalties of Hull and Propeller Roughness, *Transactions SNAME*, 89, 295-318.
Triantaphyllou, E. (2000). *Multi-Criteria Decision Making Methods*: *A Comparative Studies*, Kluwer Academic Publishers.
Trincas, G. (2001). Survey of Design Methods and Illustration of Multiattribute Decision Making System for Concept Ship Design (keynote paper). *Proceedings of MARIND 2001*, Varna, III, 21-50.
Trincas, G., Grubišić, I. and Žanić, V. (1994). Comprehensive concept design of fast ro-ro ships by multiattribute decision making. *Proceedings of 5th International Marine Design Conference, IMDC'94*, Delft, 403-418.
Trincas, G., Mauro, F., Braidotti, L. and Bucci, V. (2018). Handling the Path from Concept to Preliminary Ship Design, *Proceedings of IMDC 2018*, Espoo, Helsinki.
Ulrich, K.T. and Eppinger, S.D. (2007). *Product Design and Development*, 4th edition, Mc-Graw Hill, New York, ISBN 007123273-7.
Yoshimura, Y. and Masumoto, Y. (2011). Hydrodynamic Force Database with Medium High Speed Ships and Investigation into a Maneuvering Prediction Method, *JASNAOE*, 14, 63-73.
Yu, P.L. (1973). A Class of Solutions for Group Decision Problems, *Management Science*, 19(8), 936-946.
Zadeh, L.A. (1975). Fuzzy Sets and Their Application to Cognitive and Decision Processes, *Academic Press*.
Zeleny, M. (1982). Multiple Criteria Decision Making, *McGraw-Hill Book Company*, New York.